

Low temperature dielectric and magnetic properties of Fe-ion-doped SrTiO₃

メタデータ	言語: eng 出版者: 公開日: 2017-06-26 キーワード (Ja): キーワード (En): 作成者: メールアドレス: 所属:
URL	http://hdl.handle.net/2297/48021

Low temperature dielectric and magnetic properties of Fe-ion-doped SrTiO_3

Hideshi Fujishita^{a,*}, Yuya Arai^b, Hiroyuki Okamoto^c, Toshihisa Yamaguchi^d

^a*Institute of Liberal Arts and Science, Kanazawa University, Kanazawa, 920-1192, Japan*

^b*Division of Mathematical and Physical Sciences, Kanazawa University, Kanazawa 920-1192, Japan*

^c*School of Health Sciences, Kanazawa University, Kanazawa, 920-0942, Japan*

^d*Department of Physics, School of Science and Engineering, Meisei University, Hino, Tokyo 191-8506, Japan*

Abstract

Dielectric and magnetic properties of $\text{SrTi}_{1-x}\text{Fe}_x\text{O}_3$ were measured for a single crystal sample ($x = 0.0032$) and a ceramic sample ($x = 0.02$). Temperature dependences of the dielectric constants were analyzed on the basis of a Vendik's formula, which describes a quantum paraelectric state accurately. A small amount of Fe impurities in the single crystal does not affect the characteristic temperatures of the dielectric properties, but does affect the quality of the crystal. This change in quality causes a large change in the dielectric constant of the quantum paraelectric state. The temperature dependence of the dielectric constant of the quantum paraelectric state of the ceramic sample is different from that of the single crystal not only quantitatively, but also qualitatively. The magnetic susceptibilities obey the typical Curie law, though a deviation of the Curie law was observed below 5 K for $x = 0.02$. Crystals with the both concentrations remain in paramagnetic states at 2.5 K. The magnetic properties of $\text{SrTi}_{1-x}\text{Fe}_x\text{O}_3$ can, in all likelihood, be explained by the orientation effect of free Fe^{3+} ions. In addition, an antiferroelectric interaction suggested for EuTiO_3 by an analysis of dielectric constants based on a Barrett's formula was turned out to be unnecessary following analysis of the same data based on the Vendik's

*Corresponding author

Email address: fujishit@staff.kanazawa-u.ac.jp (Hideshi Fujishita)

formula.

Keywords: Quantum paraelectrics; Vendik model; Fe-ion-doped STO; dielectric constant; magnetic property

1. Introduction

Strontium titanate SrTiO_3 (STO) has a cubic perovskite structure of space group $\text{Pm}\bar{3}\text{m}$ at room temperature[1]. The Ti ion is surrounded by six oxygen ions, which form an octahedron in a unit cell. Sr ions occupy corners of the unit cell. STO undergoes a structural phase transition by a condensation of zone boundary R_{25} mode at 105 K [2]. The low temperature phase has a superstructure of space group I4/mcm [3]. In addition, STO shows a quantum paraelectric behavior at low temperatures. The dielectric constant of STO increases with decreasing temperature and saturates below 3 K [4]. The explanation of this has been attributed to suppression of softening of the ferroelectric optical mode coupled with other optical modes by large quantum fluctuations. This mechanism leads to a well-known expression, Barrett's formula [5]. On the basis of hyper-Raman scattering experiments, however, the quantum paraelectric state of STO was discussed to be stabilized by the structural distortion[6, 7]. Recently, we pointed out that the quantum paraelectric state is independent of the structural distortion[8]. In addition, we showed that the dielectric constant at low temperatures can be accurately described using Vendik's formula, which deals with the ferroelectric mode coupled with acoustic modes [9]. It also contains a measure of the density of defects and inhomogeneity. The low-temperature dielectric constant cannot be accurately described by Barrett's formula, even after the introduction of this measure.

To study the possibility of an enhancement of the coupling between magnetism and dielectric properties, the dielectric constant of quantum paraelectric EuTiO_3 has been measured under a magnetic field [10]. EuTiO_3 has the perovskite structure, which contains $4f$ spins of Eu^{2+} ions with $S = 7/2$ and d

itinerant electrons on the Ti^{4+} site. The enhancement is expected to occur in the quantum paraelectric state, because the energy scale of the ferroelectric soft mode is expected to be comparable with that of a magnetic interaction or magnetic field. The dielectric constant of EuTiO_3 shows a critical decrease at
30 an antiferromagnetic ordering of the Eu spins at 5.5 K. Fitting the dielectric constant below 110 K to Barrett's formula indicated the existence of antiferroelectric interaction, because of the obtained negative value of paraelectric Curie temperature T_0 .

The insulating pure STO exhibits diamagnetic behavior in addition to the
35 quantum paraelectric behavior. The localized $4f$ magnetic moments of the Eu^{3+} ions in doped STO are lower than those of the Eu^{2+} ions. However, it is still interesting to investigate the magnitude of the magnetoelectric coupling in the Eu^{3+} -doped system to obtain detailed knowledge of the coupling. Recently, these properties of $\text{Sr}_{1-3x/2}\text{Eu}_x\text{TiO}_3$ have been measured using ceramic sam-
40 ples with different Eu^{3+} doping concentrations [11]. The measured dielectric properties could be well explained by Barrett's formula. An anomalous dielectric enhancement was observed in an $x = 0.005$ sample, while dielectric suppressions were observed in other samples with greater x values. On the other hand, all the Eu doped samples exhibited doping concentration dependence of
45 paramagnetism.

Fe ions with $3d$ magnetic moments doped STO are known to replace Ti^{4+} ions in doped STO [12]. In this paper, we made dielectric and magnetic measurements of Fe-doped STO single crystal and ceramic samples to extend the understanding of the effect of Fe doping on dielectric constants and magnetic
50 coupling. Analyses of dielectric constants are performed mainly on the basis of the Vendik's formula, which describes the quantum paraelectric state accurately.

2. Experimental details

The sample of $\text{SrTi}_{0.9968}\text{Fe}_{0.0032}\text{O}_3$ used in our investigation was a Verneuil-grown crystal. A $5 \times 5 \times 0.5 \text{ mm}^3$ plate with mirror-polished (100) surfaces

55 was supplied by Furuuchi Chemical. A ceramic sample of $\text{SrTi}_{0.98}\text{Fe}_{0.02}\text{O}_3$ was prepared by means of a solid-state reaction between SrCO_3 , TiO_2 , and Fe_2O_3 , as described in Ref. [12]. A mixture with the appropriate amounts of these materials was pressed into pellets and sintered at $1200\text{ }^\circ\text{C}$ for 18 h. The pellets were reground, pressed once more into pellets, and sintered at $1400\text{ }^\circ\text{C}$ for 18 h. 60 Each pellet was cut and polished into a $5 \times 5 \times 0.5\text{ mm}^3$ plate. Electrodes with a typical area of 11.5 mm^2 were formed on the surfaces by gold evaporation for the dielectric measurements.

X-ray diffraction patterns at room temperature were measured using a Rigaku X-ray diffractometer, RINT2500, with a graphite counter monochromator and 65 an X-ray generator with a rotating Cu anode. A powder sample was obtained by grinding the ceramic samples of $\text{SrTi}_{0.98}\text{Fe}_{0.02}\text{O}_3$. The generator was operated at 50 kV and 300 mA. A diffraction pattern was measured between 20 ° and 140 ° at a scanning speed of $2\theta = 1.0\text{ }^\circ/\text{min}$. Data were collected at every $2\theta = 0.02\text{ }^\circ$. The (100) plate of single crystal $\text{SrTi}_{0.9968}\text{Fe}_{0.0032}\text{O}_3$ was adhered to a 70 powder sample holder. The generator was operated at 40 kV and 20 mA. The diffraction pattern was measured between 20 ° and 120 ° at a scanning speed of $2\theta = 2.0\text{ }^\circ/\text{min}$ in θ - 2θ mode. Data were collected at every $2\theta = 0.01\text{ }^\circ$.

The dielectric constants were measured using a precision LCR meter (HP 4284A) with an applied voltage of 500 mV. Measurements were performed for 75 both heating and cooling processes. The temperatures of the samples were controlled in the temperature region 4–325 K using a helium closed-circuit refrigerator (Daikin Industries, CG308SBR) [13]. An open-short-load correction method was adopted for the LCR meter. The sample holder was also modified to ensure more precise measurements as follows. Two pairs of co-axis cables 80 from the LCR meter, used for a four-wire method, were extended to the neighborhoods of the sample. The longer distance between the sample and the end of each pair of co-axis cables was about 3 cm.

For the magnetic properties, the temperature dependence and magnetic field dependence of magnetizations were measured using a superconducting quantum 85 interference device (SQUID) magnetometer (Quantum Design SP5000).

Least-squares fitting calculations of Vendik's formula were performed using a computer program Gnuplot, where a recursive definition technique was employed for an integral function; no approximate expressions of the integral function were used. We also performed least-squares fitting calculations of Barrett's formula using another computer program KaleidaGraph.

3. Results

X-ray diffraction patterns of $\text{SrTi}_{0.9968}\text{Fe}_{0.0032}\text{O}_3$ and $\text{SrTi}_{0.98}\text{Fe}_{0.02}\text{O}_3$ are delineated in Fig. 1(a) and (b), respectively. The patterns were measured at room temperature to ascertain that there were no impurity peaks or structural changes caused by Fe-ion doping. Diffraction indices (hkl) are given taking a perovskite unit cell of space group Pm3m. Because a (100) plate of single crystal was used for the former pattern, only the peaks with ($h00$) can be observed in Fig.1(a). The patterns show that the doping did not cause impurity phases or structural changes. Fig. 2 indicates the dielectric constant ε (real part) of $\text{SrTi}_{1-x}\text{Fe}_x\text{O}_3$ as a function of temperature at a frequency of 10 kHz measured for the (a) single crystal with $x = 0.0032$ along the direction [100] and (b) ceramic sample with $x = 0.02$.

Magnetic susceptibilities measured at a magnetic field of 0.02 T are delineated in Fig. 3 as a function of temperature for the (a) single crystal with $x = 0.0032$ and (b) ceramic sample with $x = 0.02$.

Figure 4 shows the magnetic hysteresis curves measured at 2.5 K for the (a) single crystal with $x = 0.0032$ and (b) ceramic sample with $x = 0.02$.

4. Analysis and discussion

Temperature dependencies of dielectric constant ε (real part) of $\text{SrTi}_{1-x}\text{Fe}_x\text{O}_3$ have been analyzed on the basis of Barrett's formula and Vendik's formula. A normalized bias field, ξ_B , and a measure of density of defects and inhomogeneity, ξ_S , were introduced to Barrett's formula in the same form, $\xi^2 = \xi_B^2 + \xi_S^2$, as appears in Vendik's formula.

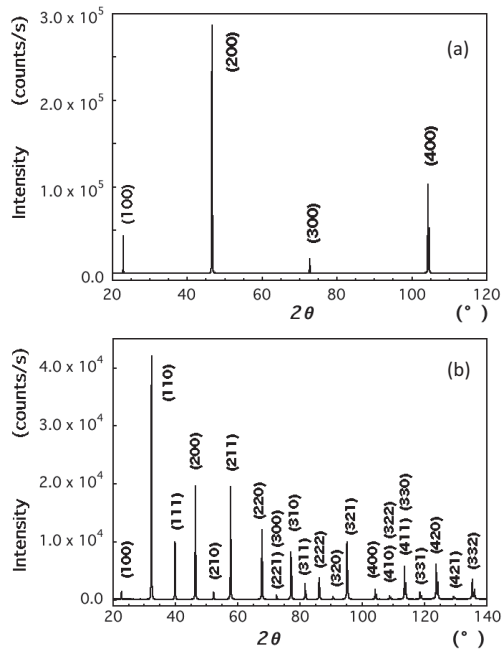


Figure 1: X-ray diffraction patterns of (a) $\text{SrTi}_{0.9968}\text{Fe}_{0.0032}\text{O}_3$ and (b) $\text{SrTi}_{0.98}\text{Fe}_{0.02}\text{O}_3$ measured at room temperature. A (100) plate of single crystal was used for (a), while a powder sample was used for (b). Diffraction indices (hkl) are given taking a perovskite unit cell of space group $\text{Pm}\bar{3}\text{m}$.

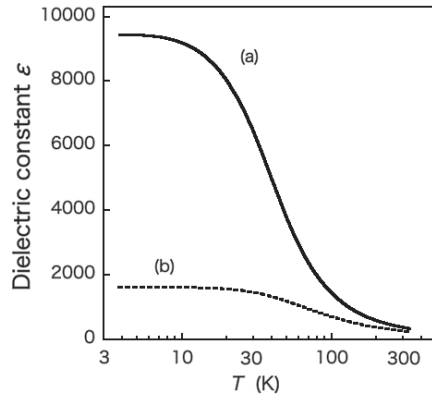


Figure 2: Dielectric constant ϵ (real part) of $\text{SrTi}_{1-x}\text{Fe}_x\text{O}_3$ as a function of temperature measured at a frequency of 10 kHz for (a) single crystal with $x = 0.0032$ along [100] and (b) ceramic sample with $x = 0.02$.

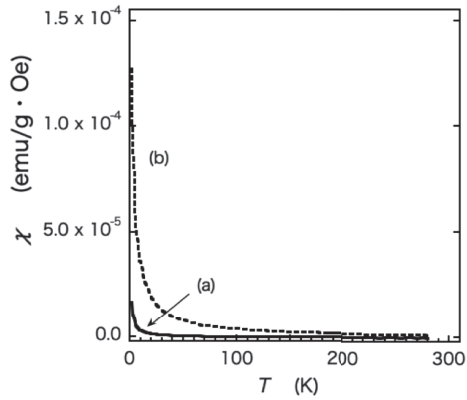


Figure 3: Magnetic susceptibility of $\text{SrTi}_{1-x}\text{Fe}_x\text{O}_3$ as a function of temperature measured at a magnetic field of 0.02 T for (a) single crystal with $x = 0.0032$ and (b) ceramic sample with $x = 0.02$.

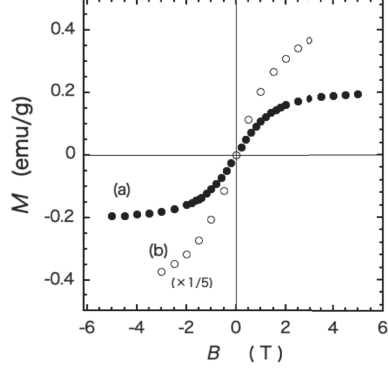


Figure 4: Magnetic hysteresis curve of $\text{SrTi}_{1-x}\text{Fe}_x\text{O}_3$ measured at 2.5 K for (a) single crystal with $x = 0.0032$ and (b) ceramic sample with $x = 0.02$.

$$\varepsilon(T) = \frac{C/T_0}{[\sqrt{\xi^2 + \eta^3 + \xi}]^{2/3} + [\sqrt{\xi^2 + \eta^3 - \xi}]^{2/3} - \eta} + \varepsilon_0, \quad (1)$$

where C is a Curie constant, T_0 is a paraelectric Curie temperature, and ε_0 is a temperature-independent constant, which is not included in the original formula. ξ_B was set at 0 in the present study. η in Barrett's formula is written as

$$\eta = \frac{T_1}{2T_0} \coth\left(\frac{T_1}{2T}\right) - 1, \quad (2)$$

where T is the sample temperature and $k_B T_1$ is an energy of other optical modes that couples with the ferroelectric optical mode. k_B is the Boltzmann constant. Eqs. (1) and (2) agree with the original Barrett's formula for $\xi = 0$ and $\varepsilon_0 = 0$. η in Vendik's formula is written as

$$\eta = \frac{T_D}{2T_0} \left[\frac{1}{2} + \frac{2}{(T_D/T)^2} \int_0^{T_D/T} \frac{x}{e^x - 1} dx \right] - 1, \quad (3)$$

where $k_B T_D$ is the highest energy of acoustic modes that couples with the ferroelectric mode.

The results of fitting these formulae to the data for the single crystal $\text{SrTi}_{1-x}\text{Fe}_x\text{O}_3$ with $x = 0.0032$ are shown in Fig. 5 (a) and Table I. Our previous results [8] for a pure single crystal SrTiO_3 are indicated in the figure by blue circles, and blue and black lines for comparison. The obtained values are compared in Table I. Fig. 5 (b) indicates the result of fitting the formulae to the data for the ceramic sample $\text{SrTi}_{1-x}\text{Fe}_x\text{O}_3$ with $x = 0.02$. The result obtained for pure ceramic SrTiO_3 by Yu *et al.*[11] is delineated by the blue broken line in Fig. 5 (b) for comparison. The blue broken line was produced using the values obtained by fitting Barrett's formula to their observations, where the value of C was changed to 7.95×10^4 K from 7.01×10^4 K in Table 2 of Ref. [11] to reproduce the maximum ε value of 2000 in Fig. 3(a) of Ref. [11].

Table 1: Comparison of values obtained for single crystal $\text{SrTi}_{1-x}\text{Fe}_x\text{O}_3$ by fitting Vendik's formula. The numbers in parentheses indicate the standard errors. The values for $x=0$ were obtained in our previous work [8].

$\text{SrTi}_{1-x}\text{Fe}_x\text{O}_3$	C (K) $\times 10^4$	T_D (K)	T_0 (K)	ε_0	ξ
$x = 0$ (Ref. [8])	7.91 (5)	281 (2)	67.1 (5)	5 (2)	0.0098 (3)
$x = 0.0032$ (present)	7.735 (7)	281.6 (3)	63.84 (8)	67.3 (2)	0.0277 (2)

The maximum value of the dielectric constant of the single crystal with $x = 0.0032$ was half that of the pure single crystal ($x=0$). In spite of such a difference, the characteristic temperatures, C , T_D , and T_0 , are almost equal. The difference in the maximum values of the dielectric constants is caused by the three-fold difference in ξ , the measure of the density of defects and inhomogeneity, which was brought about by the doping with Fe ions. The dielectric constants of the ceramic with $x = 0.02$ are different from those of single crystals not only in their temperature dependence but also in their maximum values as follows:

1. The temperature dependence of ε obtained for $x = 0.02$ can be fitted well by both the Vendik's and Barrett's formulae. The fitted curves were almost similar. The characteristic temperatures obtained changed moderately from those obtained for the single crystal with $x = 0.0032$. However,

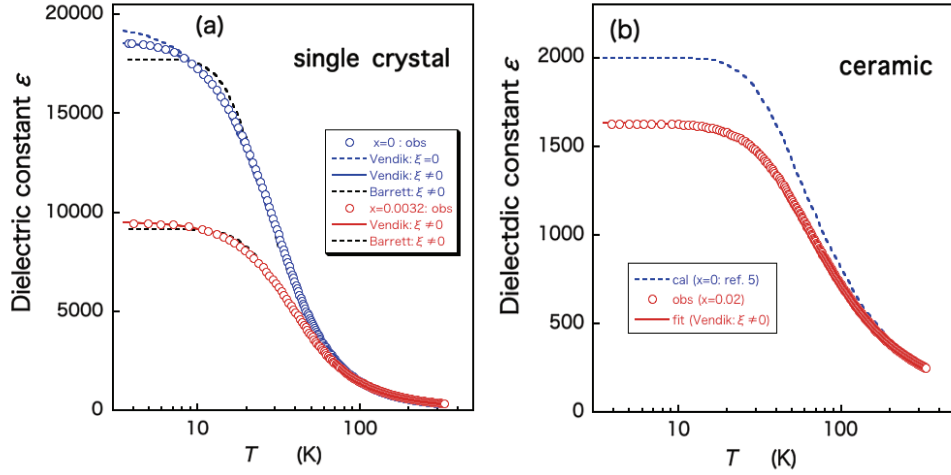


Figure 5: (a) Comparison of fittings of Vendik's formula (red solid line) and Barrett's formula (black broken line) to the dielectric constant ε (real part) of single crystal $\text{SrTi}_{1-x}\text{Fe}_x\text{O}_3$ with $x = 0.0032$ along [100] measured at 10 kHz, where red open circles are plotted at every 50 data points. The blue open circles indicate our previous data for pure single crystal SrTiO_3 [8]. The blue broken and solid lines are the results of fitting Vendik's formula with $\xi=0$ or $\xi\neq 0$, respectively. The black broken line is the result of fitting Barrett's formula with $\xi\neq 0$. (b) Result of fitting Vendik's formula (red solid line) to the dielectric constant ε (real part) of ceramic $\text{SrTi}_{1-x}\text{Fe}_x\text{O}_3$ with $x = 0.02$ measured at 10 kHz, where observed data (red open circles) are plotted at every 10 data points. Blue broken line indicates the data of pure ceramic SrTiO_3 measured by Yu *et al.*[11]. The line was produced using the values obtained by fitting Barrett's formula to their observations (see text).

ξ changed drastically, to 38.9 and 27.6, respectively, which are 1400 times and 125 times of those for the single crystal with $x = 0.0032$, respectively.

150

2. The maximum value of the dielectric constant of the ceramic sample with $x = 0.02$ was less than 1/11 times that of the pure single crystal ($x = 0$). However, the maximum value of the ceramic sample with $x = 0$ (blue broken line in Fig. 5(b)) by itself is about 1/9 times that of the pure single
155 crystal.

160

165

The results obtained for single crystals are more reliable than those for ceramic samples, with regard to not only their temperature dependences, but also the maximum values of their dielectric constants. In contrast to an enhancement of the maximum value of the dielectric constant after doping the ceramic sample with small amounts of Eu, the maximum value of the dielectric constant is found to decrease with 2 % Fe doping of the ceramic sample. The reason for this is that the characteristic temperatures of 2% Fe-doped ceramic change significantly in contrast to the case of the single crystal with 0.32 % Fe doping, although the temperature values for 2% Fe-doped ceramic sample are less reliable because of the extremely large values of ξ .

170

175

Fig. 6 shows magnetic susceptibilities of $\text{SrTi}_{1-x}\text{Fe}_x\text{O}_3$ as a function of inverse temperature measured at 0.02 T for the single crystal with $x = 0.0032$ (solid circles) and the ceramic sample with $x = 0.02$ (open circles), where susceptibilities for solid circles are enlarged five times. The susceptibilities for $x = 0.0032$ obey the typical Curie law, in contrast to the results for $\text{Sr}_{1-3x/2}\text{Eu}_x\text{TiO}_3$ and the diamagnetic behavior of pure SrTiO_3 . Magnetic hysteresis curves measured at 2.5 K (Fig. 4) indicate that both systems remain in a paramagnetic state at 2.5 K. Magnetic moments in units of μ_B per Fe ion are shown in Fig. 7 as a function of B/T , where μ_B is the Bohr magneton. A broken line delineates the calculated magnetic moment caused by the orientation effect of a Fe^{3+} free ion ($J = 5/2$, where J is the total angular momentum) using a Brill-

loun function. The observed values were well proportional to the calculation, though the proportional constants for $x = 0.032$ and $x = 0.02$ were 0.4 and 0.64, respectively. The magnetic properties of $\text{SrTi}_{1-x}\text{Fe}_x\text{O}_3$ can, in all likelihood, be explained by the orientation effect of free Fe^{3+} ions, in contrast to the mechanism for the Eu^{3+} case with $J = 0$.

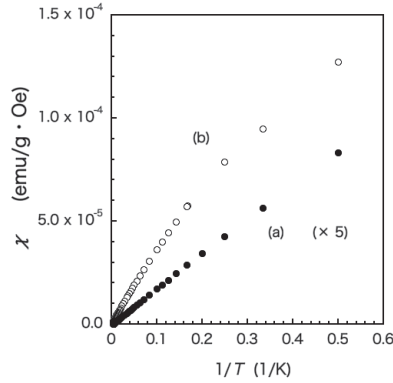


Figure 6: Magnetic susceptibility of $\text{SrTi}_{1-x}\text{Fe}_x\text{O}_3$ as a function of inverse of temperature measured at 0.02 T for (a) single crystal with $x = 0.0032$ and (b) ceramic sample with $x = 0.02$.

The quantum paraelectric perovskite EuTiO_3 , which contains Eu^{2+} ions with $J = S = 7/2$, shows antiferromagnetic ordering of the Eu spins at 5.5 K. The dielectric constant shows a critical decrease below 5.5 K [10]. Antiferroelectric interaction was suggested to exist, because Barrett’s formula with negative value of $T_0 = -25$ K could be fitted well to the dielectric constant between 5.5 and 100 K, although no additional anomalies associated with the interaction could be detected between 5.5 and 100 K.

To evaluate this analysis, dielectric constants were reproduced first on the basis of Barrett’s formula using the values obtained from the fitting: The dielectric constants were calculated by Eqs. (1) and (2) with $C = 2.34 \times 10^4$ K, $T_1 = 162$ K, $T_0 = -25$ K, $\varepsilon_0 = 181$, and $\xi = 0$, which are shown in Fig. 8 by open circles. These dielectric constants were analyzed by Vendik’s formula, Eqs. (1)

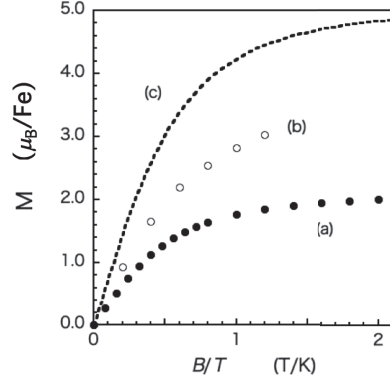


Figure 7: Magnetic hysteresis curve of $\text{SrTi}_{1-x}\text{Fe}_x\text{O}_3$ per Fe ion measured at 2.5 K for (a) single crystal with $x = 0.0032$ and (b) ceramic sample with $x = 0.02$. Broken line (c) is a calculated curve for a Fe^{3+} free ion using a Brillouin function. μ_B is the Bohr magneton.

195 and (3). The result of the fitting is shown by the line in Fig. 8, which explains the reproduced values well. The obtained values were $C = 1.33 (5) \times 10^4$ K, $T_D = 141 (5)$ K, $T_0 = 0.7 (20)$ K, $\varepsilon_0 = 223 (3)$, and $\xi = 8.5 (390) \times 10^2$. A positive T_0 value was obtained, which means the no existence of antiferroelectric interaction, though the error range for T_0 was very large.

200 5. Conclusions

A small amount of Fe impurities in single crystal of $\text{SrTi}_{1-x}\text{Fe}_x\text{O}_3$ does not affect the characteristic temperatures of dielectric properties, but does affect the quality of the crystals. This change in quality causes a large change in the dielectric constant of the quantum paraelectric state. Temperature dependence of the dielectric constant of the quantum paraelectric state of the ceramic sample is different from that of the single crystal not only quantitatively, but also qualitatively. This indicates that the dielectric constants of ceramic samples observed in quantum paraelectric states are less reliable compared to those observed in single crystals. The magnetic susceptibilities for $x = 0.0032$ and 0.02 obey the typical Curie law, though deviation from the Curie law was observed below 5 K

205

210

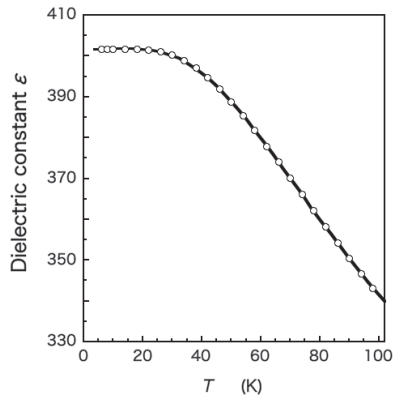


Figure 8: Dielectric constant of single crystal EuTiO_3 as a function of temperature below 100 K. Open circles were obtained by calculations on the basis of values given in Ref. [10] (see text). The line is a fit of Vendik's formula.

for $x = 0.02$. Crystals with both concentrations remain in paramagnetic states at 2.5 K. The magnetic properties of $\text{SrTi}_{1-x}\text{Fe}_x\text{O}_3$ can, in all likelihood, be explained by the orientation effect of free Fe^{3+} ions. An antiferroelectric interaction suggested for EuTiO_3 by the analysis of dielectric constants based on the Barrett's formula turned out to be unnecessary after analysis of the same data using Vendik's formula.

- [1] R. A. Cowley, Phys. Rev. **134**, 1964, A981-A997.
- [2] G. Shirane and Y. Yamada, Phys. Rev. **177**, 1969, 858-863.
- [3] H. Fujishita, Y. Shiozaki, and E. Sawaguchi, J. Phys. Soc. Jpn. **46**, 1979, 581-586.
- [4] K. A. Müller and H. Burkard, Phys. Rev. B **19**, 1979, 3593-3602.
- [5] J. H. Barrett, Phys. Rev. **86**, 1952, 118-120.
- [6] H. Vogt, Phys. Rev. B **51**, 1995, 8046-8059.

- 225 [7] A. Yamanaka, M. Kataoka, Y. Inaba, K. Inoue, B. Hehlen, and E. Courtens, Europhys. Lett. **50**, 2000, 688-694.
- [8] H. Fujishita, S. Kitazawa, M. Saito, R. Ishisaka, H. Okamoto, and T. Yamaguchi, J. Phys. Soc. Jpn. **85**, 2016, (074703-1-8).
- [9] O. G. Vendik and S. P. Zubko, J. Appl. Phys. **82**, 1997, 4475-4483.
- [10] T. Katsufuji and H. Takagi, Phys. Rev. B **64**, 2001, (054415-1-4).
- 230 [11] J. Yu, L. Fang, T. Cai, S. Ju, W. Dong, F. Zheng, and M. Shen, J. App. Phys. **111**, 2012, (063529-1-6).
- [12] D.P. Fagg, V.V. Kharton, A.V. Kovalevsky, A.P. Viskup, E.N. Naumovich, and J. R. Frade, J. Eur. Ceram. Soc. **21**, 2001, 1831-1835, (for example).
- [13] T. Yamaguchi and S. Sawada, J. Phys. Soc. Jpn. **60**, 1991, 3162-3166.